

ANALYTICAL AND EXPERIMENTAL HEAT TRANSFER AND FLOW-
FIELD PREDICTION ON A RECTANGULAR REENTRY MODULE

A. L. LAGANELLI
Senior Scientist
Science Applications, Inc.
Wayne, Pa. 19087

MASTER

PRESENTATION:

AIAA Aerothermal Workshop

Session II: Utilization of Wind Tunnel Data

Place: Colorado Springs, Co.

March 17, 1980

ACKNOWLEDGEMENT

This work was sponsored by the Department of Energy
and performed under contract to the General Electric Company -
Space Division.

AC01-79ET32043

There is no objection from this to the
public release or
dissemination of the document(s)

Noted in this file

SAFETY INVESTIGATION GROUP

2/22/80 J. C. H.

MOW

DISCLAIMER

This book was prepared at the cost of work sponsored by an agency of the United States Government.
Neither the United States Government nor any agency thereof nor any of their employees makes any
warranty, express or implied, or assumes any liability or responsibility for the accuracy,
completeness, or usefulness of any information, apparatus, product, or process disclosed or
represented that it does not infringe privately owned rights. Reference herein to any specific
commercial product, process, or service by trade name, trademark, manufacturer, or otherwise does
not necessarily constitute or imply its endorsement, recommendation, or favoring by the United
States Government or any agency thereof. The views and opinions of authors expressed herein do not
necessarily state or reflect those of the United States Government or any agency thereof.

DISCLAIMER

This report was prepared as an account of work sponsored by an agency of the United States Government. Neither the United States Government nor any agency Thereof, nor any of their employees, makes any warranty, express or implied, or assumes any legal liability or responsibility for the accuracy, completeness, or usefulness of any information, apparatus, product, or process disclosed, or represents that its use would not infringe privately owned rights. Reference herein to any specific commercial product, process, or service by trade name, trademark, manufacturer, or otherwise does not necessarily constitute or imply its endorsement, recommendation, or favoring by the United States Government or any agency thereof. The views and opinions of authors expressed herein do not necessarily state or reflect those of the United States Government or any agency thereof.

DISCLAIMER

Portions of this document may be illegible in electronic image products. Images are produced from the best available original document.

NOMENCLATURE

| | |
|---------------------------|--|
| a | speed of sound - ft/sec. |
| b | GPHS width - ft. |
| c_p | specific heat - BTU/lbm °R |
| C_p | pressure coefficient |
| C_{H_0} | defined by Equation (A-15) |
| h | enthalpy - BTU/lbm |
| k_r | roughness height - ft. |
| K_L | laminar augmentation heating factor |
| l | GPHS length - ft. |
| M | Mach number |
| p | pressure - psf |
| Pr | Prandtl number |
| q | heat transfer - BTU/Ft ² -Sec. |
| r_{eff} | effective radius - ft. |
| R_N, R_C, R_B | radius of spherical nose, corner, body - ft. |
| Re | Reynolds number |
| s | wetted length - ft. |
| T | absolute temperature - °R |
| u, v | velocity, axial and normal - ft/sec. |
| $\partial u / \partial s$ | velocity gradient - 1/sec. |

Greek Symbols

| | |
|----------|---|
| α | angle of attack - degrees |
| β | velocity gradient parameter $(D/u_\infty)(du/ds)_0$ |
| γ | specific heat ratio c_p/c_v |

NOMENCLATURE (Continued)

δ^* boundary layer displacement thickness - ft.

ϵ_L laminar compressibility factor

θ momentum thickness - ft.

μ viscosity - lbm/ft-sec.

ρ_0 defined by Equation (A-14)

ρ density - lbm/ft³

Subscripts

$s,0$ stagnation point values

GPSH General Purpose Heat Source

FFC flat faced cylinder

e boundary layer local conditions

cw cold wall conditions

w wall conditions

2 based on conditions behind a normal shock

tr transition

0 based on momentum thickness

∞ freestream conditions

Superscripts

0 total conditions

* based on reference enthalpy conditions

ANALYTICAL AND EXPERIMENTAL HEAT TRANSFER AND FLOWFIELD PREDICTION ON A RECTANGULAR REENTRY MODULE

A. L. Laganello
Senior Scientist
Science Applications, Inc.
Wayne, Pa.

INTRODUCTION

A General Purpose Heat Source (GPHS) has been designed for the purpose of supplying power to a radioisotope thermal generator intended for interplanetary missions. The baseline configuration, nominally 2 inch x 4 inch x 4 inch with sharp edges and corners, is required to survive accidental earth reentry as well as terminal impact velocities. Several problems have been identified relative to survival criteria during reentry that include the module motion and the associated heat transfer. The present paper will be concerned with flow field and reentry heating for a broad face-on (4 inch x 4 inch) or side-on (2 inch x 4 inch) reentry orientation. Moreover, the analysis will consider convective heat transfer in the absence of roughness or ablation effects during the supersonic/hypersonic regime of reentry.

In order to assess the structural/thermal behavior of the GPHS module, an understanding of flow field and subsequent boundary conditions is required. Since the basic "brick" aeroshell design has not received any attention in past literature, experimental data on related shapes has been used to assess the required heat transfer characteristics (boundary conditions for a conduction heat transfer code). Data of this type are extremely limited and prediction capability has resorted to semi-empirical techniques and data correlations.

The objective of the present study is to determine the flow field characteristics and subsequent local properties on the GPHS configuration to obtain heating levels during hypersonic/supersonic reentry. This analysis will be compared to semi-empirical techniques based on wind tunnel data.

A schematic representation of the flow field distribution about the GPHS configuration during a broad face-on stable reentry mode is shown in Figure 1. The bow shock is detached from the body by a value of Δ . The flow expands toward the sharp corner and decompresses to the adjacent side reaching sonic conditions at the corner. The flow further expands toward the base region and dissipates into the wake behind the module.



SCIENCE APPLICATIONS, INC.

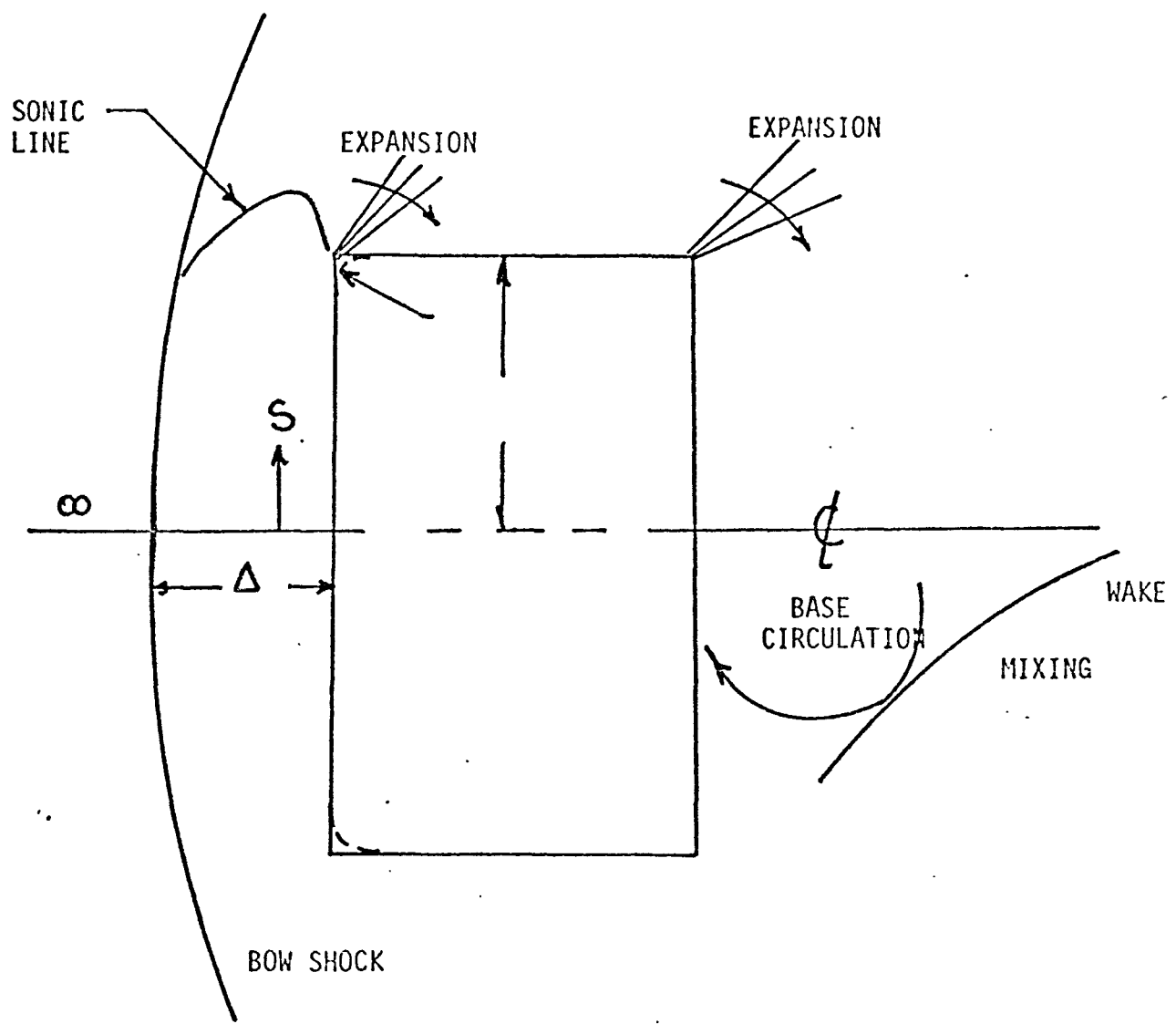


FIG. 1. FLOW FIELD ON GPHS BROAD SIDE REENTRY

Since the GPHS module poses a difficult reentry shape to analyze, experimental data featuring flat faced walls with flow expansion over sharp corners was used to determine the heat flux levels. The distribution was determined by Eq. (1) where the ratio q_w/q_o , config. was obtained from wind tunnel results. Flat faced circular and hexagonal cylinder data provided some definition of the heat transfer distributions. These data are available from several sources^{1,2,3}. The stagnation heat transfer value was obtained from an expression that relates a hemispherical value to the brick shape GPHS through an area aspect ratio given by Eq. (2). Here, b and l represent the width and length of the module, respectively. The velocity gradient term is represented as the ratio of a flat faced cylinder to that of a sphere and has been taken to be 0.565. The remaining terms represent the Mangler factor (axisymmetric flow) and the area aspect ratio. The stagnation heating for the sphere is that developed by Detra, et al⁴ for hypersonic flow conditions ($M > 5$).



SCIENCE APPLICATIONS, INC.

WIND TUNNEL DATA TECHNIQUE

$$\dot{\bar{g}}_w = \left(\frac{\dot{\bar{g}}_w}{\dot{\bar{g}}_{0, \text{GPHS}}} \right) \dot{\bar{g}}_{0, \text{GPHS}} \quad (1)$$

CALCULATED
BASED ON TUNNEL DATA

$$\frac{\dot{\bar{g}}_{0, \text{GPHS}}}{\dot{\bar{g}}_{0, \text{sphere}}} = \frac{1}{\sqrt{2}} \sqrt{\frac{(\partial u / \partial s)_{0, \text{FFC}}}{(\partial u / \partial s)_{0, \text{sph.}}}} \sqrt{\frac{R_{N, \text{sph}}}{b/2}} \left[1 + \left(\frac{b}{l} \right)^{1/2} \right]^{1/2} \quad (2)$$

MANGLER
MANAGER
FACTOR

VELOCITY
GRADIENT

AREA ASPECT
RATIO

$$\dot{\bar{g}}_{0, \text{sph.}} = \frac{17600}{\sqrt{R_N}} \sqrt{\frac{\rho_{\infty}}{\rho_{SL}}} \left(\frac{V_{\infty}}{26000} \right)^{3.15} \quad (3)$$

Figure 2 shows a compilation of experimental and theoretical stagnation point velocity gradients taken from Perini⁵. One observes that the ratio 0.565 used by previous analyst can be in error for values of Mach number less than 5. Perini suggested the following empirical curve fit for the velocity gradient of a sphere and flat faced cylinder; namely:

$$\beta_{FFC} = \left. \frac{\partial u}{\partial s} \right)_0 \frac{D}{U_\infty} = 0.29 + \frac{0.983 (1+M_\infty^2)^{3.12}}{1+M_\infty^3} \quad (4)$$

and

$$\beta_{Sphere} = \left. \frac{\partial u}{\partial s} \right)_0 \frac{D}{U_\infty} = 1.10 + \frac{1.56}{(1+M_\infty^2)^{.79}} \quad (5)$$

For a rectangular shape such as the GPHS, wind tunnel data will be required to determine the velocity gradient. However, the flat faced cylinder will be used as a first order approximation.

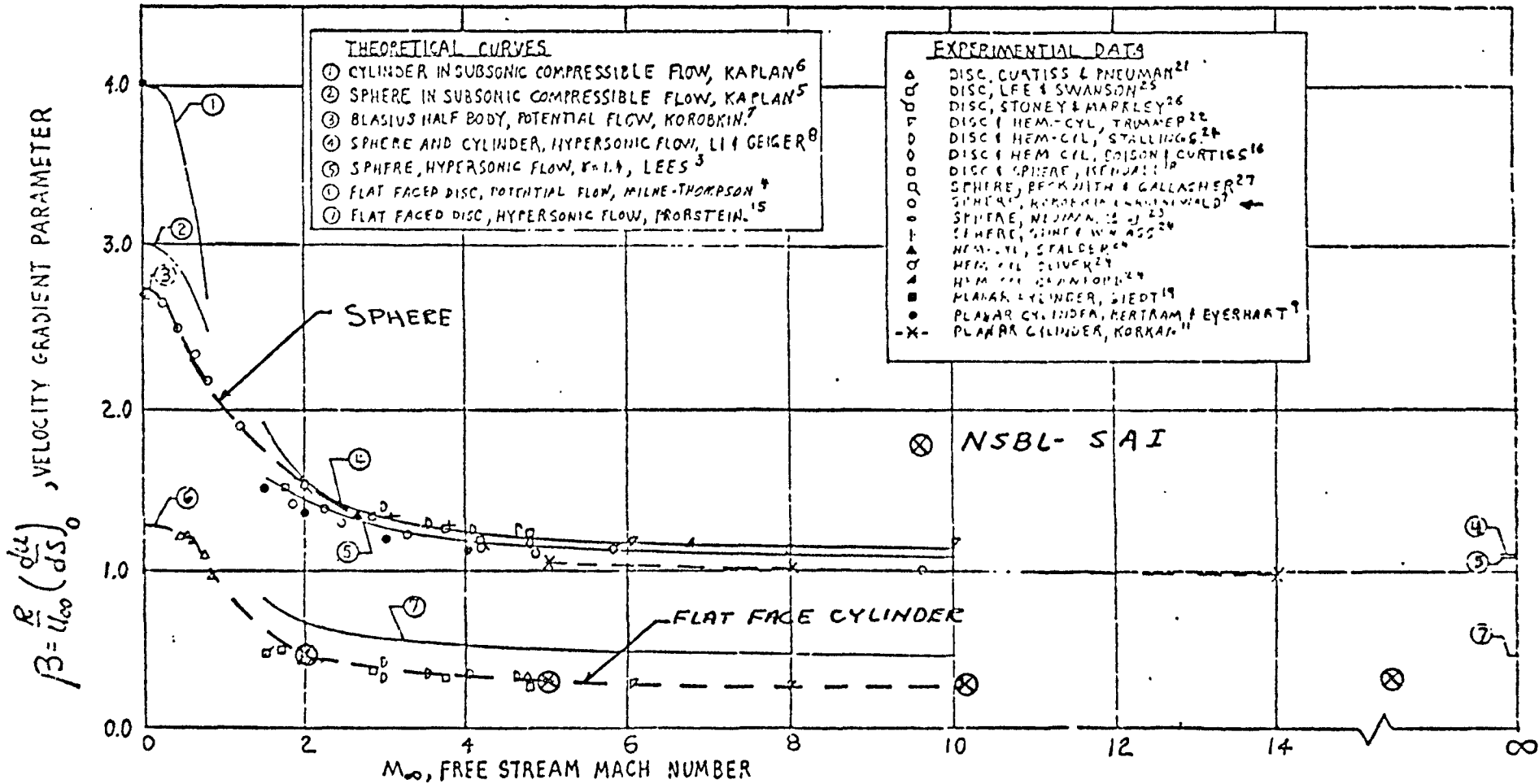


FIG. 2 COMPILATION OF EXPERIMENTAL AND THEORETICAL STAGNATION POINT VELOCITY GRADIENTS (REF. 5)

REFERENCE SPHERE HEAT TRANSFER

Calculation of the reference sphere stagnation heat flux value gives the heat flux distribution as a function of altitude (time) for a specific trajectory. Detra, et al⁴ correlation was based on the classic work of Fay and Riddell⁶ together with experimental (shock tube) data. However, the use of Eq. (6) for $M < 5$ is questionable as a consequence of property evaluation⁷. On the other hand, Lees⁸ considered a highly cooled boundary layer for $M \gg 1$ ($h_e \gg h_w$) and comparison of Eqs. (6) and (7) indicated that the latter yielded values 20 to 30% higher. Consequently, Lee's result was modified to include a reference enthalpy to account for property variations with compressibility (given as Eq. (8)). It is recommended that Eq. (8) be used for $M < 5$.



SCIENCE APPLICATIONS, INC.

REFERENCE SPHERE HEAT TRANSFER

Detra et al⁴

$$\dot{q}_{0, \text{sphere}} = \frac{17600}{\sqrt{R_N}} \sqrt{\frac{\rho_\infty}{\rho_s}} \left(\frac{u_\infty}{26000} \right)^{3.15} \left(\frac{h_e - h_w}{h_e - h_w \text{ at } 300K} \right) \quad (6)$$

Lees¹⁸

$$\dot{q}_{0, \text{sphere}} = \frac{1}{2} \sqrt{2} \Pr^{-2/3} \sqrt{\rho_e / \mu_e} \sqrt{(du/ds)_0} (h_e - h_w) \quad (7)$$

$$\dot{q}_{0, \text{sphere}} = \frac{1}{2} \sqrt{2} \Pr^{-2/3} \sqrt{\rho_e / \mu_e} \epsilon_0 \sqrt{(du/ds)_0} (h_e - h_w) \quad (8)$$

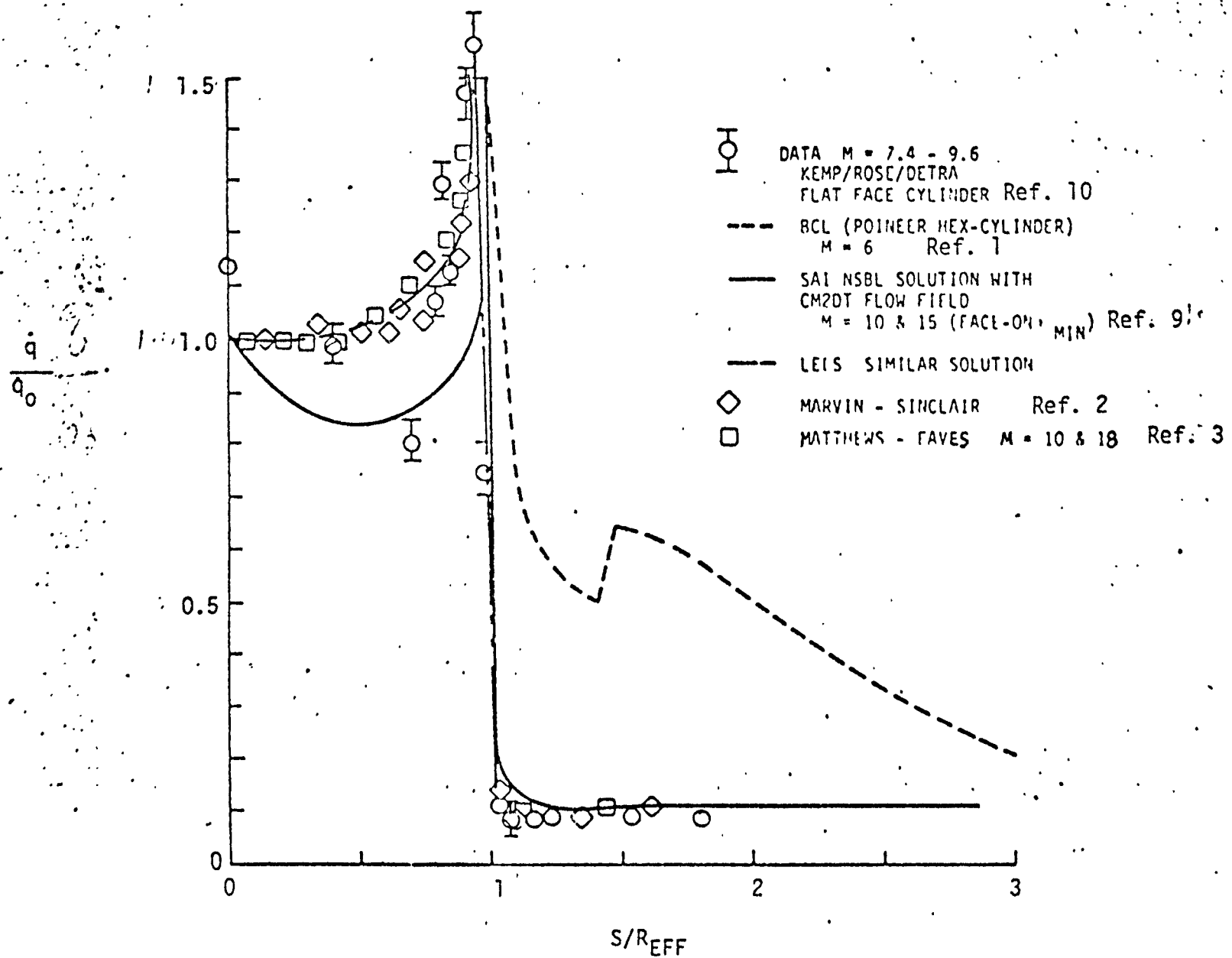
$$\epsilon_0 = \sqrt{\frac{\rho^* \mu^*}{\rho_e \mu_e}}$$

$$h^* = \frac{1}{2} (h_e + h_w) \quad @ s=0$$

$$\frac{du}{ds}_0 = \frac{u_\infty}{R_N} \left[\frac{\rho_\infty}{\rho_s} \left(2 - \frac{\rho_\infty}{\rho_s} \right) \right]^{1/2}$$

Figure 3 shows the heat flux distribution for a flat faced straight and hexagonal cylinder for both similar (Lees)⁸ and non-similar solutions⁹. The hexagonal cylinder data indicate a higher level of heat transfer along the adjacent wall than the straight cylinder data of References 2, 3 and 10. It should be noted that the straight cylinder data considered several corner radii as well as sharp corners. Moreover, the hexagonal cylinder data was obtained from a surface paint technique and data reduction was rendered questionable. It is possible that the higher levels were a consequence of flow separation and boundary layer transition.

FIG. 3. COMPARISON OF DATA WITH NSBL PROGRAM AND CM2DT FLOW FIELD



NON-SIMILAR BOUNDARY LAYER SOLUTION - FLOW FIELD

Figure 4-1 shows the pressure distribution predicted by the SAI CM2DT flow field code. The solution considered the GPHS module to be approximated as a flat-faced cylinder with finite corner radius. The assumption of a finite corner radius is required to avoid singularities that would be present at a sharp corner. The CM2DT code¹¹ solves the time dependent Euler equations using a second-order accurate finite-difference technique, and obtains the steady flow solution as the asymptotic limit of the time-dependent problem. The output of CM2DT provides a definition of the flow properties throughout the shock layer, as well as definition of bow shock shape and surface properties. As can be seen in Figure 4-1, the variations of the solutions with decreasing corner radius are becoming smaller as the corner radius approaches 0.0625. Thus, this value of the corner radius was accepted as a valid approximation to the sharp corner case.

Boundary layer calculations on the GPHS module are performed using the implicit finite-difference solution of the axisymmetric compressible boundary layer equations described by Blottner¹². For these viscous calculations, it is necessary to provide definition of the boundary layer edge conditions from the inviscid (CM2DT) analyses. For $M > 1$, the information required includes both a surface pressure distribution and a bow shock shape (b.l. edge entropy is calculated through a mass balance procedure). Figure 4-2 shows the results of the normalized heat flux distribution at several Mach numbers for a given trajectory.

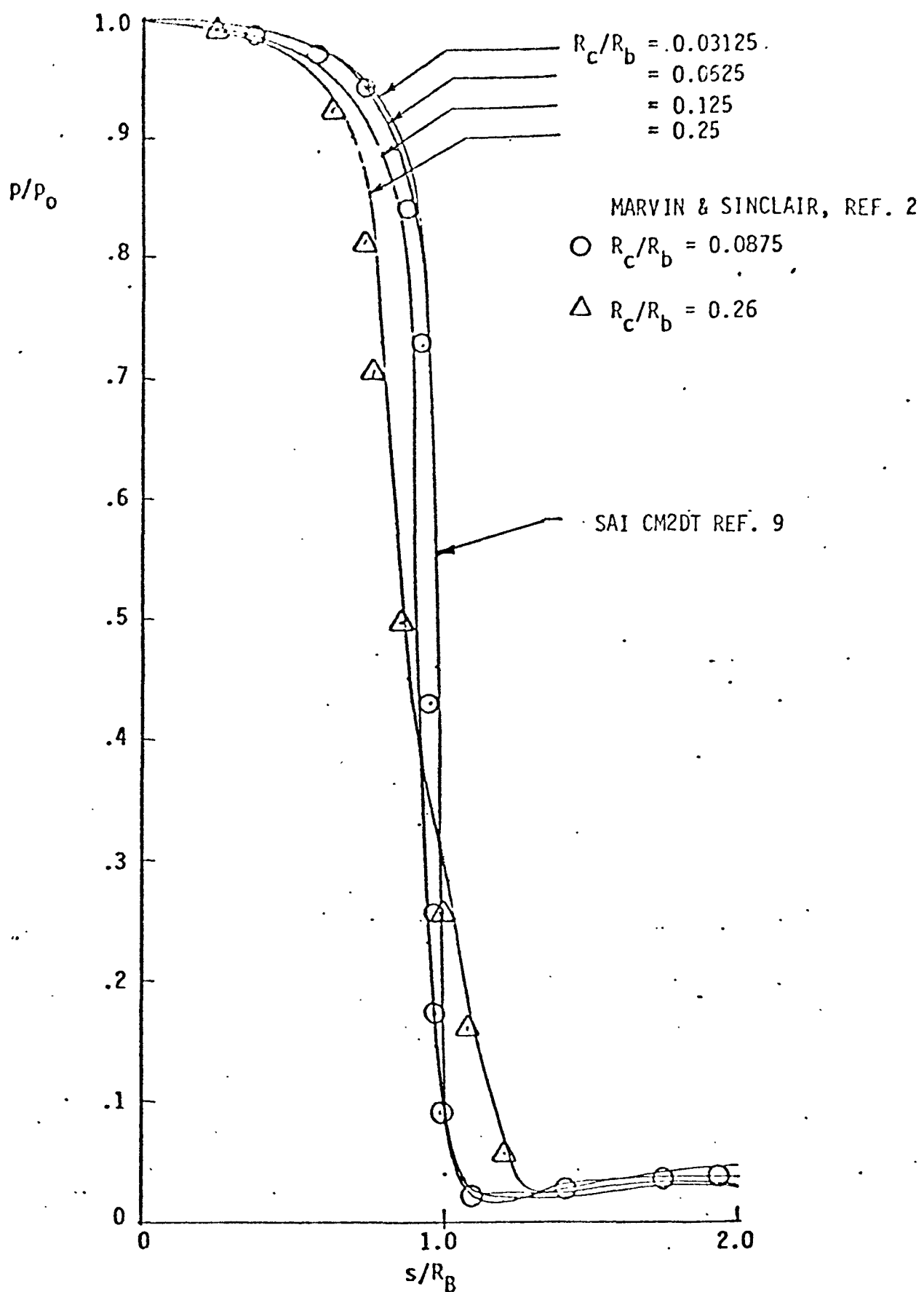


FIGURE 4.1. GPHS MODULE SURFACE PRESSURE DISTRIBUTION, $M_\infty = 10$

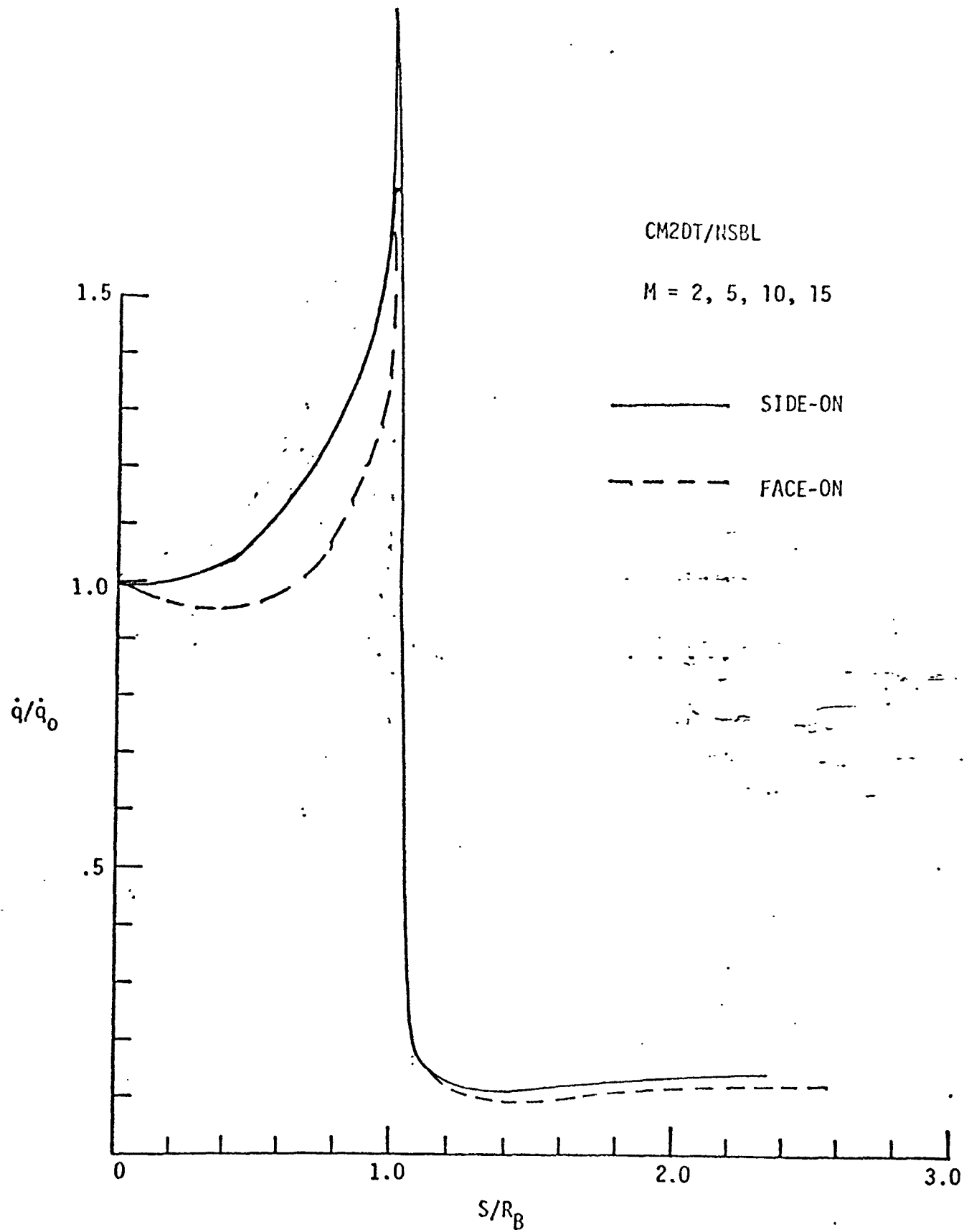


FIG. 4-2. NORMALIZED HEAT TRANSFER DISTRIBUTION

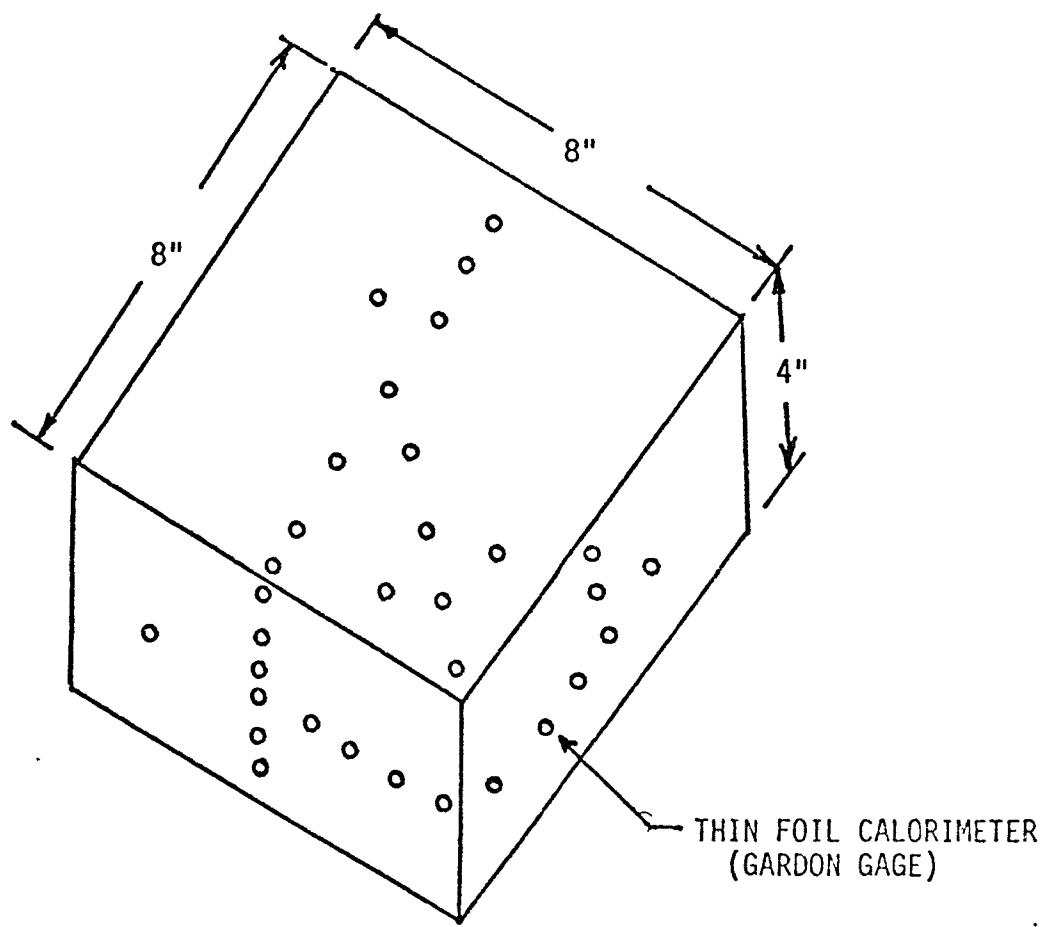
WIND TUNNEL TEST PROGRAM

A wind tunnel test program was conducted on the GPHS module (twice scale) at the AEDC von Karman Tunnel B facility at Mach 8. The Reynolds number was fixed (nominally at 1.33×10^6) and the model was subject to several angles of attack at four positions. The model was instrumented on four forces using thin foil calorimeters (Gardon type heat gages). The broad face (8" x 8") and side face (4" x 8") results will be given at $\alpha = 0^\circ$. Oil flow tests were also made to observe flow characteristics at the model edges. Three dimensional effects were observed along the model sides/edges.



SCIENCE APPLICATIONS, INC.

WIND TUNNEL TEST MODEL



AEDC von KARMAN TUNNEL B

$M = 8$

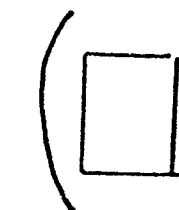
$T_{\infty}^{\circ} = 1265^{\circ}\text{R}$

$Re_{\infty}/\text{ft} = 1.33 \times 10^6$

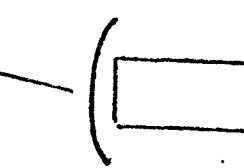
$0 \leq \alpha \leq 110^{\circ}$

POSITIONS

○ FACE-ON



○ SIDE-ON



○ EDGE-ON

○ CORNER-ON

Figure 5 shows the normalized heat flux distribution at zero angle of attack along the four faces containing instrumentation. The data are shown compared to the SAI non-similar solutions. It appears that the side-on distribution reflects slightly higher levels than the face-on values. This is believed to be a consequence of the 3-D effects of the 4" x 8" face compared to the 2-D, 8" x 8" face area. Moreover, a significant increase in heat transfer is evident as the sonic line (model edge) is approached. The distribution yields very low values as the flow turns the sharp corner during expansion (decompression). In any event, theory appears to predict the heat flux distribution for the complex shape.

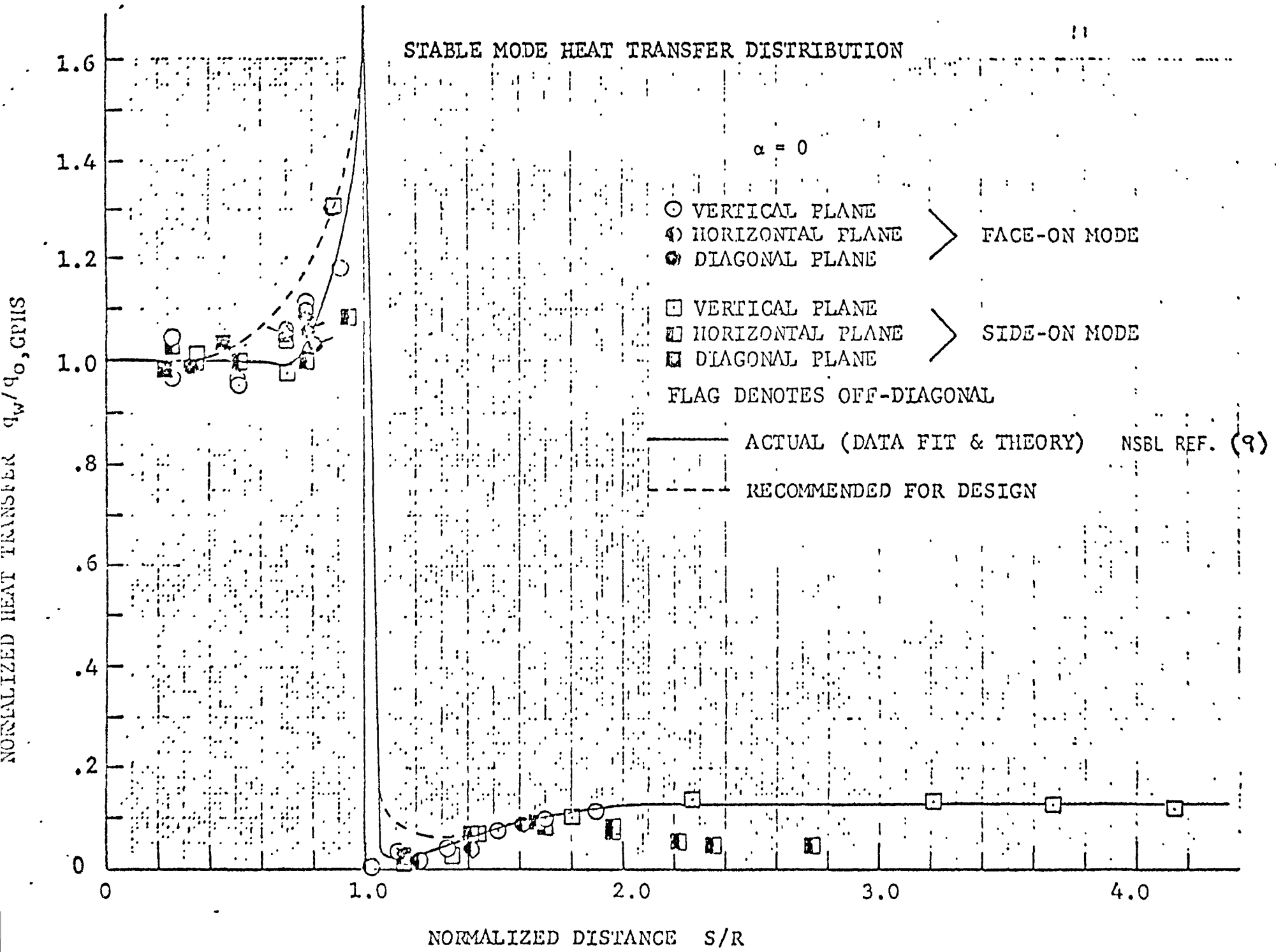


FIGURE 5. GPHS STABLE MODE HEAT TRANSFER DISTRIBUTION

CONCLUSIONS

- Heat transfer distributions for non-circular shapes can be obtained for reentry conditions using wind tunnel data for the surface distributions and a stagnation value based on a reference sphere condition. The distributions obtained at a fixed Mach number ($M > 1$) appear valid over an extended range of Mach numbers.
- The above requires
 - (1) definition of a proper velocity gradient
 - (2) definition of an area aspect ratio
- Flowfield predictions (inviscid) using the CM2DT program provide a proper definition of pressure and shock characteristics for non-similar (viscous) solutions.

REFERENCES

1. "Final Safety Analysis Report," Vol. I, Teledyne Isotopes Energy Systems Division, Report ESD-3069-15-2.
2. Marvin, J. G., and Sinclair, A. R., "Convective Heating in Regions of Large Favorable Pressure Gradient," AIAA J., 5, 11, 1940-1942, November 1967.
3. Matthews, R. K., and Eaves, R. H., Jr., "Comparison of Theoretical and Experimental Pressure and Heat Transfer Distributions on Three Blunt Nosed Cylinders in Hypersonic Flow," AEDC-TR-67-148, ARO, September 1967.
4. Detra, R. W., Kemp, N. J. and Riddell, F. R., "Addendum to - Heat Transfer to Satellite Vehicles Re-entering the Atmosphere," Jet Propulsion, November 1957, p. 1256.
5. Perini, L. L., "Compilation of Experimental Stagnation Point Velocity Gradients and Heat Transfer Data on Subsonic and Supersonic Flow," Applied Physics Laboratory Report AED-75-29, ANSP-068A, August 1975.
6. Fay, J. A. and Riddell, F. R., "Stagnation Point Heat Transfer in Dissociated Air," AVCO Report 1, April 1957.
7. Laganelli, A. L., "Erosion/Ablation Systems Analysis Program," G. E. Document No. 73SD2162, September 1973.
8. Lees, L., "Laminar Heat Transfer Over Blunt-Nosed Bodies at Hypersonic Flight Speeds," Jet Propulsion, Vol. 26, No. 4, April 1956.
9. Laganelli, A. L. and Hall, D. W., "Flow Field Modeling of GPHS During Reentry," SAI Report SAI-067-80R-003, October 1979.
10. Kemp, N. H., Rose, P. H., and Detra, R. W., "Laminar Heat Transfer Around Blunt Bodies in Disassociated Air," J. of Aero. Sci., Vol. 26, p. 421, 1959.
11. Hall, D. W., "Calculation of Inviscid Supersonic Flow over Ablated Nosetips," AIAA Paper No. 79-0342, January 1979.
12. Blottner, F. G., "Finite-Difference Methods of Solution of the Boundary Layer Equations," AIAA J., 8, 2, 193-205, February 1970.